Aleksandar Sedmak[1], Aleksandar Grbović[1], Radzeya Zaidi[1], Snežana Kirin[2], Nikola Vitas[3], Tamara Golubović[4], Ivana Vučetić[2]

NUMERICAL, ANALYTICAL AND EXPERIMENTAL DETERMINATION OF REMAINING LIFE OF A PIPE WITH AN AXIAL CRACK

NUMERIČKO, ANALITIČKO I EKSPERIMENTALNO ODREĐIVANJE PREOSTALOG VEKA CEVI SA OSNOM PRSLINOM

Originalni naučni rad / Original scientific paper
UDK /UDC:

Rad primljen / Paper received: 20.08.2023

Adresa autora / Author's address:
[1)] University of Belgrade, Faculty of Mechanical Engineering, Serbia *email: aleksandarsedmak@gmail.com
[2)] University of Belgrade, Innovation Centre of the Faculty of Mechanical Engineering, Belgrade, Serbia
[3)] Ministry of Economy, Belgrade, Serbia
[4)] University of Belgrade, Innovation Centre of the Faculty of Technology and Metallurgy, Belgrade, Serbia

Keywords
- axial crack
- extended finite element method
- Paris law
- API J55 steel

Ključne reči
- aksijalna prslina
- proširena metoda konačnih elemenata
- Parisov zakon
- API J55 čelik

Abstract

Numerical and analytical methods are applied to determine the remaining life of oil rig pipe with an axial crack. Analytical expressions for surface cracks are used to calculate stress intensity factors for different crack geometries and estimate the remaining life directly by using Paris law. The same procedure is applied by using the FEM, verified previously by experimental results. Good agreement between analytical and numerical results is demonstrated.

Izvod

Primenjene su numeričke i analitičke metode za određivanje preostalog veka cevi naftne platforme sa aksijalnom prslinom. Analitički izrazi za površinske prsline korišćeni su za izračunavanje faktora intenziteta napona za različite geometrije prsline i za procenu preostalog veka korišćenjem Parisovog zakona. Isti postupak je primenjen korišćenjem MKE, prethodno verifikovan eksperimentom. Pokazano je dobro slaganje analitičkih i numeričkih rezultata.

INTRODUCTION

In general, cracks are the most significant threat to structural integrity, including pipelines, /1, 2/. Evaluation of the defects is important for pipeline companies because some pipelines perhaps become defective during service periods, as explained in more detail in /3-5/. One can say that the more the pipeline ages, the more integrity assessment is required, including risk based approach, /6-11/.

Another problem is fatigue crack growth, starting from a microscopic formation of a crack, all the way to the critical size, and eventual failure. Therefore, pipelines as pressure equipment must be designed and constructed to guarantee safety and security in exploitation. Welded pipes in oil and gas wells are highly responsible structures, so it is important to know their resistance to fracture and fatigue. Using parameters of fracture mechanics, obtained based on experimental research, an estimate of remaining life of oil rig pipe with an external axial surface crack can be made by using the analytical calculation in a relatively simple way. At the same time, amplitude stress and crack size effects on the remaining fatigue life can be determined, /12-13/. This is also possible by using the extended finite element method (XFEM), as already shown /2, 12/ and done in this paper. Prior to this, the finite element method (FEM) has been verified by experimental results, as shown in /12/.

ANALYTICAL CALCULATION USING PARIS LAW

A schematic presentation of the cracked pipe is shown in Fig. 1. Basic data for the HF welded pipe with an axial crack, made of API J55 steel, Fig. 1, are as follows:
- diameter 139.7 mm; thickness 6.98 mm; length 702 mm,
- pressure, maximum 10.1 MPa, minimum 7.89 MPa,
- number of strokes of pump rod: n_{PR} = 9.6 min^{-1}.

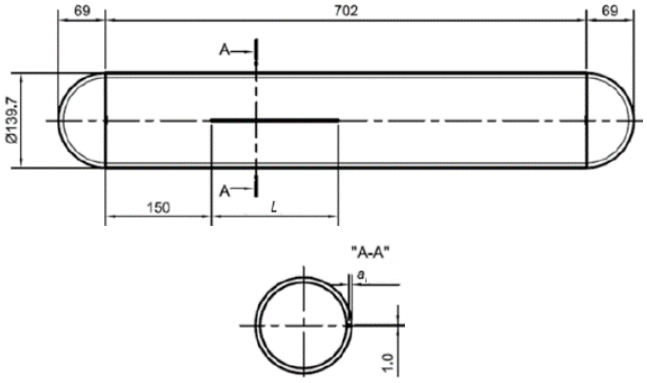

Figure 1. Dimensions of pipe and crack, /2, 3/.

The axial surface crack is made on the outer surface with length 2c = 200 mm and depth a = 3.5 mm. It is located in the base metal, i.e., in the region with the lowest values of fracture toughness, /2, 3/. Now one can use the Paris law,

$$\frac{da}{dN} = C(\Delta K)^m = C\left(Y\left(\frac{a}{W}\right)\Delta\sigma\sqrt{\pi a}\right)^m, \qquad (1)$$

where: $Y(a/W)$ is the geometry factor depending on crack length and geometry (component width); ΔK is stress intensity factor range corresponding to stress amplitude $\Delta\sigma$ = 21.2 MPa, to calculate fatigue crack growth, first into depth, and then along pipe length, /2, 6/. For the first phase of crack growth, i.e., its growth into depth, the initial length (depth) was 3.5 mm, with final lengths 4.19, 4.88, 5.57, and 6.26 millimeters, to be used in the directly integrated value of the number of cycles:

$$N = \frac{2}{(m-2)C\left(Y(a/W)\Delta\sigma\right)^m \pi^{m/2}}\left(\frac{1}{a_0^{\frac{m-2}{2}}} - \frac{1}{a^{\frac{m-2}{2}}}\right), \qquad (2)$$

where: C and m denote real data obtained by tests, C = 2.11×10^{-15}, m = 6.166 for the used material, /2, 3/. The geometry coefficient $Y(a/W)$ is taken as 3.791 for surface crack (length 200 mm, depth 3.5 mm), /14, 15/, without changing its value during crack growth. Calculated number of cycles N is shown in Fig. 2 for defined values of crack depth a.

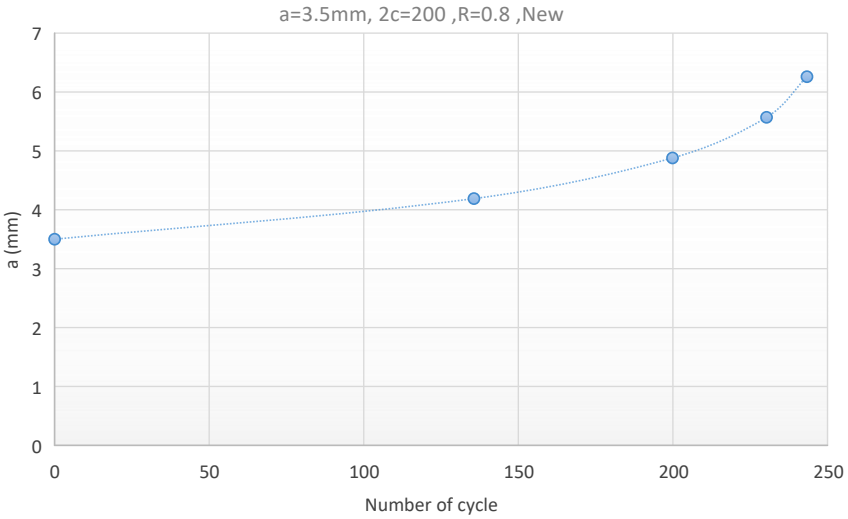

Figure 2. Crack depth vs. number of cycles.

EXTENDED FINITE ELEMENT METHOD (XFEM)

The geometry used in the simulation is based on the pipe shown in Fig. 1, with crack length $2c$ = 200 and depth a = 3.5 mm. Finite element mesh is shown in Fig. 3a, modelling half of the pipe due to symmetry.

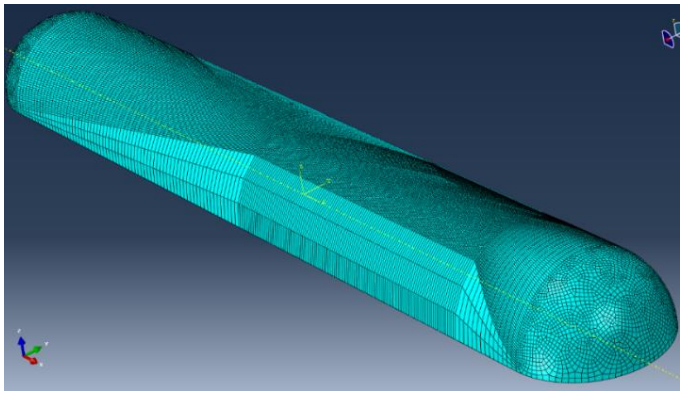

Figure 3a. Pipe model with initial axial surface crack.

Abaqus was used with hexahedral type elements, Fig. 2, consisting of 286033 nodes and 257560 elements. In the area where the crack is expected to increase a much denser network is generated. Figure 3b shows the initial crack on the pipe and the mesh in its immediate vicinity. The growth simulation was 0.2 mm in free crack propagation option. However, the crack grew a step chosen by Morfeo/Crack for Abaqus© itself, based on calculated values of the stress intensity factor, so that crack growth per step is very different. In the first 6 steps increments were 0.69 mm, while from the seventh step further a few millimeters.

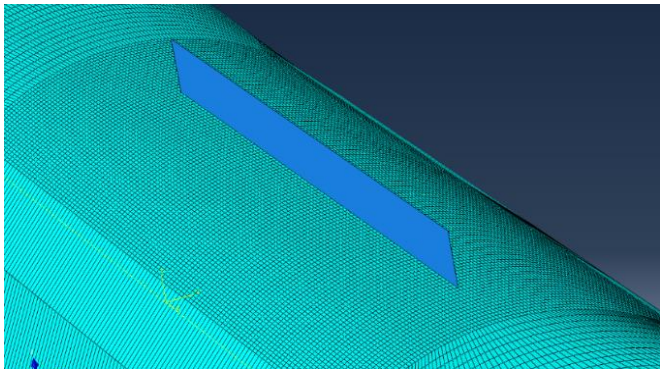

Figure 3b. Finite element mesh with an initial axial surface crack.

Three-dimensional crack growth simulation was done for a total of 100 steps so that final crack length was 209.42 mm. The crack growth option used was free crack growth. The first step in the analysis of crack growth using XFEM is 'opening' crack (no growth) and stresses in the pipe are calculated and based on stress intensity factors at the top of the crack, and the angle of deflection in relation to the initial direction of the crack is determined. Figure 4 shows the mesh in the 1st step, while other steps are shown in /6/.

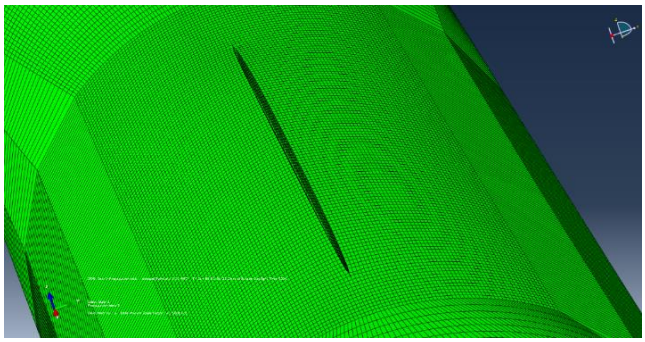

Figure 4. FE mesh in the first step of 'opening' of the crack.

The appearance of the pipe from the inside and the von Mises stress in the area around crack steps 1 and 3 are shown in Fig. 5. In the third step, a crack appeared on the inside of the pipe, 68.24 mm long, but the crack had not yet opened, Fig. 5b. In the 7th step, a crack opened on the inside of the pipe. Figure 6 shows a newly formed through crack on the inner half of the wall, 25.88 mm long. Following the direction of the outer initial axial crack (Fig. 6b, the length of the 'open' crack was $2c$ = 120 mm). More details, including 3D chart of crack growth and stress intensity factor dependence on crack growth steps are given in /2, 6, 12/.

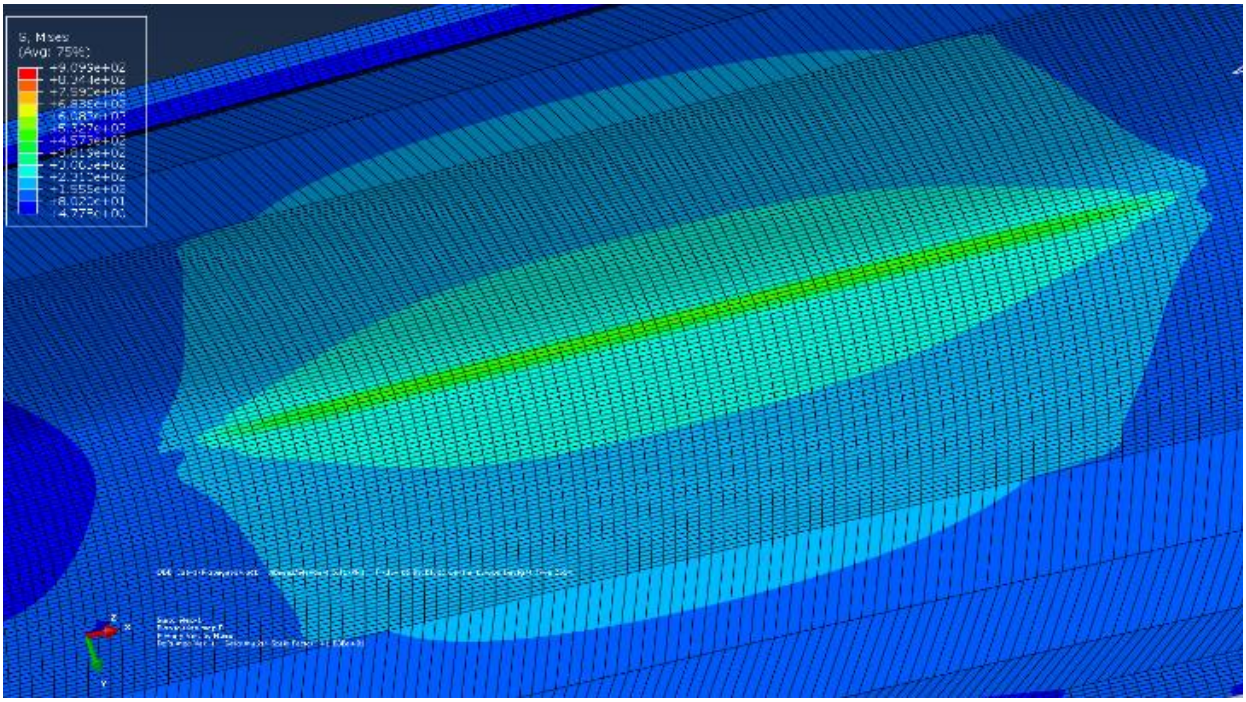

Figure 5a. 1st step - crack opening (view from inner side).

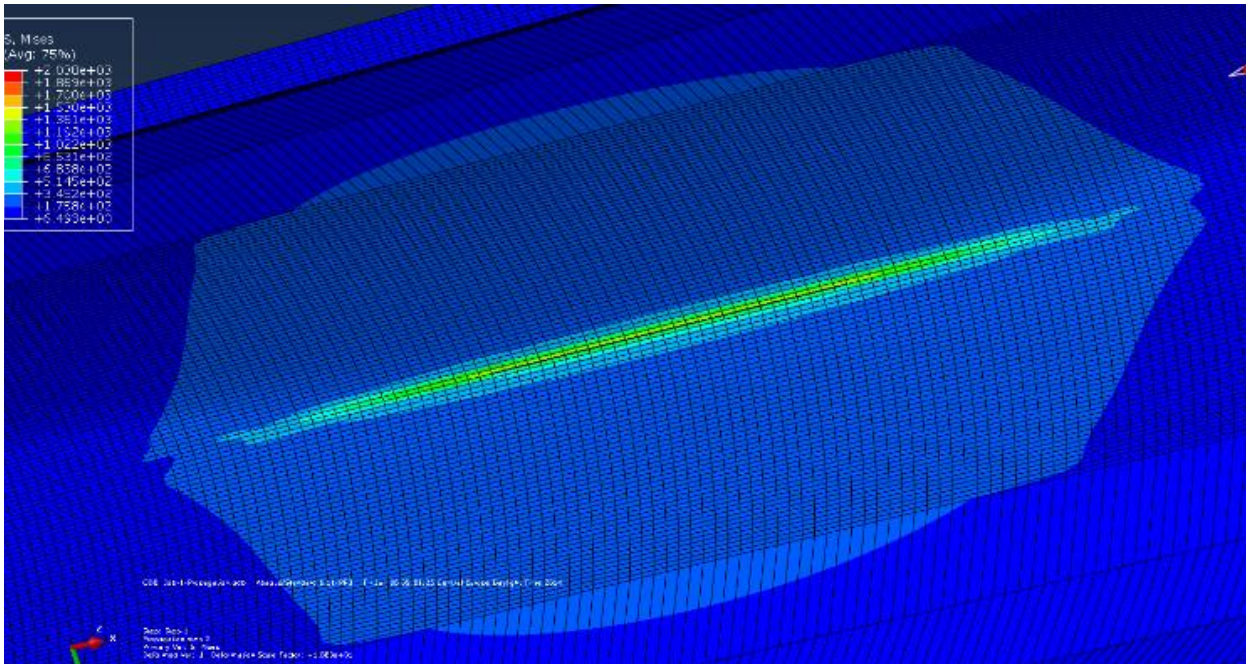

Figure 5b. 3rd step - appearance of a crack on the inside.

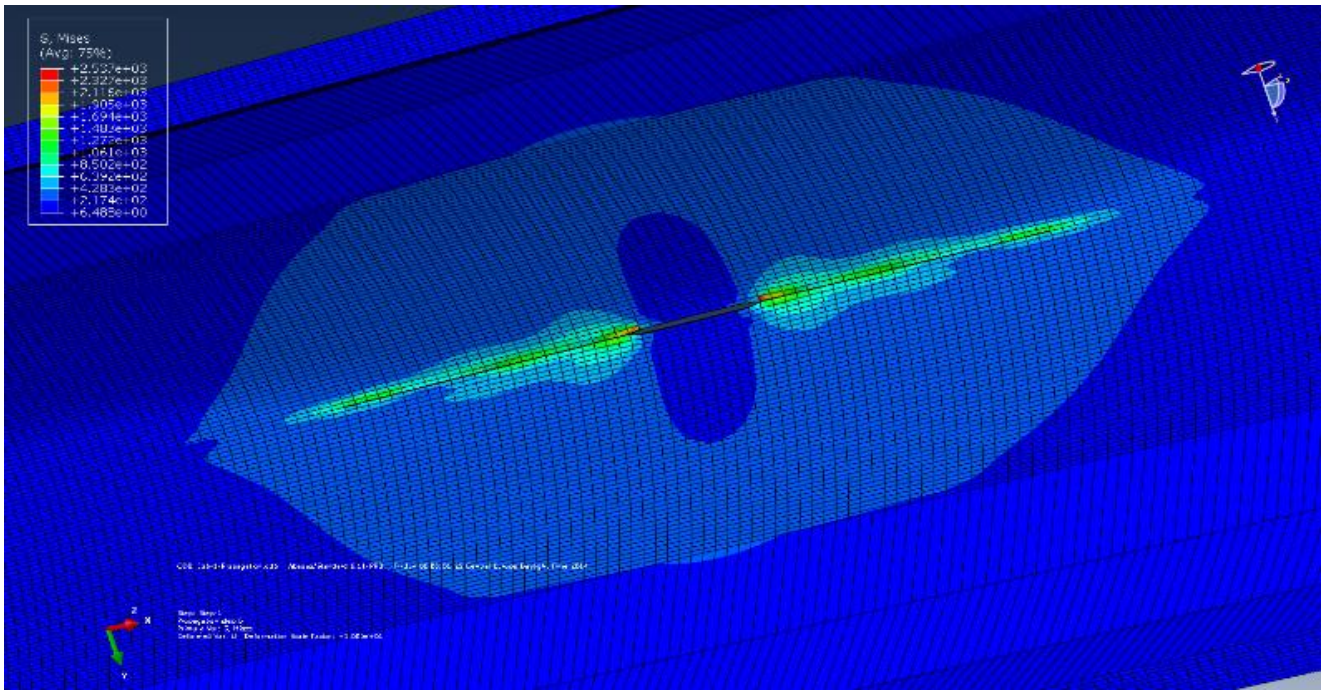

Figure 6a. Crack appearance from the bottom in the seventh step (the crack 'passes' through the pipe wall).

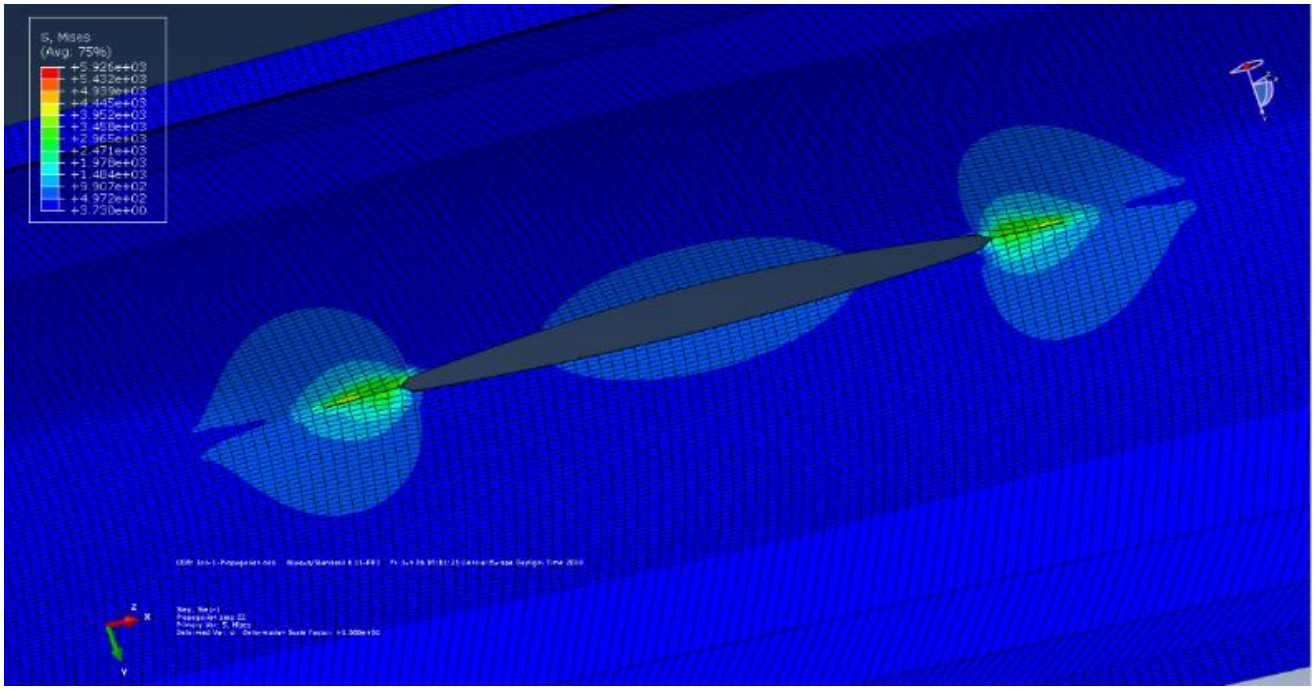

Figure 6b. Crack appearance on the inside of the pipe and von Mises stresses in the 23rd propagation step.

In the following, obtained values of stress intensity factor are considered by 3D simulation stresses calculated at a large number of points along crack front, Table 1. Values of stress intensity factor are shown in the last four columns, respectively, the equivalent stress intensity factor K_{eq}, and stress intensity factors for modes I, II, and III (K_I, K_{II}, and K_{III}). It is obvious that stress intensity factor (SIF) values for mode I are much higher than for modes II and III. Hence, it makes sense to further predict the crack growth rate by considering only values of K_I, or even better K_{eff} because it takes into account the stress intensity factors of all three modes. Table 2 shows the number of simulation steps, total crack length, number crack front points, as well as values (minimum, maximum and mean) for stress intensity factor mode I (K_I) and equivalent stress intensity factor (K_{eq}) for some characteristic simulation steps.

For crack growth through depth, the initial length (depth) was 3.5 mm, with final lengths 4.19, 4.88, 5.57, and 6.26 mm, as was the case for analytical calculations. Results are shown in Fig. 7, as crack depth vs. number of cycles for easy comparison with analytical results. As one can see, the number of cycles for each crack depth are smaller than the analytical ones (215 vs. 243 of K_c for 6.26 mm crack depth). This somewhat unexpected result is probably the conse-

quence of underestimated stress intensity factor by analytical expressions, as a typical problem for relatively long cracks. More details can be found in /2/.

When the crack penetrates the pipe wall, in the 7th step, it becomes an axial through crack 25.88 mm long (on the inside of the wall) and continues to grow only in axial direction, following the external initial crack. The total number of cycles for the crack to grow from 200 mm initial length and 3.5 mm depth to a final length of 209.42 mm was 258 cycles, part of which the crack grew until it became transient 25.88 mm long (7th step) and consumes the largest part, 229 cycles. Figure 8 shows the dependence of total crack length *a* vs. number of cycles *N* required for the crack to grow to a final length of 209.42 mm. The blue line indicates the crack that occurs on the inside of the pipe wall, which grows in the radial direction until the sixth step, and then begins to develop very quickly in the axial direction to a length of 200 mm (from 25.88 to 200 mm only about 225 cycles are required). Crack growth is then somewhat slower, up to 209.42 mm of length (required only about 30 cycles). It is obvious that the largest number of cycles was needed for the crack to rise in the first seven steps, until it broke through the pipe wall, because then the crack front was the largest. The pink line in the diagram in Fig. 8 represents an initial axial crack 200 mm long on the outside of the wall.

Table 1. Software provided values for each crack growth step.

curves. abscissa along the crack front	X (coord. data point front)	*y*	*z*	K_{eq}	K_{I}	K_{II}	K_{III}
0	50.7745	8.77E-05	69.4784	860.175	837.413	1.55444	1.65058
0.349	50.7745	8.72E-05	69.1294	859.6	837.004	1.468	1.74059
0.698	50.7745	8.68E-05	68.7804	859.072	836.648	1.38001	1.83133
1.047	50.7745	8.64E-05	68.4314	858.595	836.348	1.29048	1.92288
1.396	50.7745	8.59E-05	68.0824	858.175	836.113	1.19942	2.01528
1.745	50.7745	8.55E-05	67.7334	857.82	835.95	1.10692	2.1085
2.094	50.7745	8.51E-05	67.3844	857.54	835.868	1.01306	2.20247

Table 2. Equivalent stress intensity factor and stress intensity factor mode I.

			equivalent stress intensity factor			*stress intensity factor* mode I		
step	crack length (mm)	number of front points	max	min	mean value	max	min	mean value
1	3.5	206	1870.06	856.863	1363.462	1896.53	835.868	1366.199
2	4.19	208	2194.46	880.989	1537.725	2198.72	853.959	1526.34
3	4.88	208	2431.09	916.345	1673.718	2432.93	885.092	1659.011
4	5.57	208	2727.92	921.732	1824.826	2745.87	900.343	1823.107
5	6.26	208	2813.96	921.732	1875.125	2984.54	900.343	1948.814
6	6.9	207	3367.18	960.857	2164.019	3647.07	936.596	2291.833
7	25.883	185	7433.56	798.383	4115.972	6959.8	769.833	3864.817
8	40	173	7566.9	769.35	4168.125	7639.73	740.371	4190.051
18	101.179	119	10098.7	672.668	5385.684	9770.31	629.367	5199.839
23	120	106	10565.3	736.698	5650.999	10176.3	679.722	5428.011
47	171.769	60	10918.9	3146.38	7032.64	10498.1	2982.88	6740.49
59	190.593	45	7859.79	5479.08	6669.435	7337.13	3747.14	5542.135
64	200	45	7431.78	5903.18	6667.48	7710.26	5916.5	6813.38
71	200	49	7314.96	6272.92	6793.94	7060.96	6277.72	6669.34
100	209.417	50	7341.33	6323.69	6832.51	7201.13	5681.02	6441.075

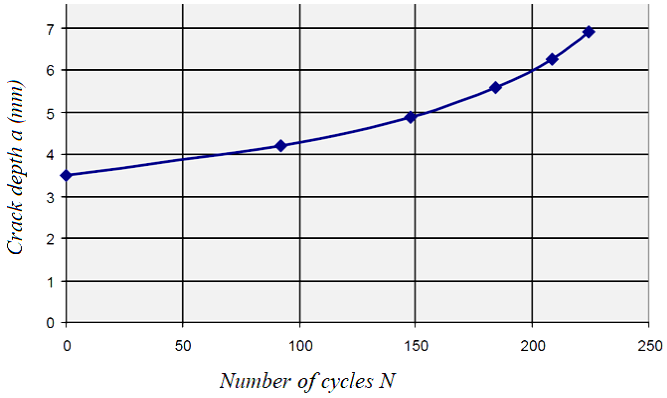

Figure 7. Crack propagation into the depth of pipe wall (first 6 steps) until penetration.

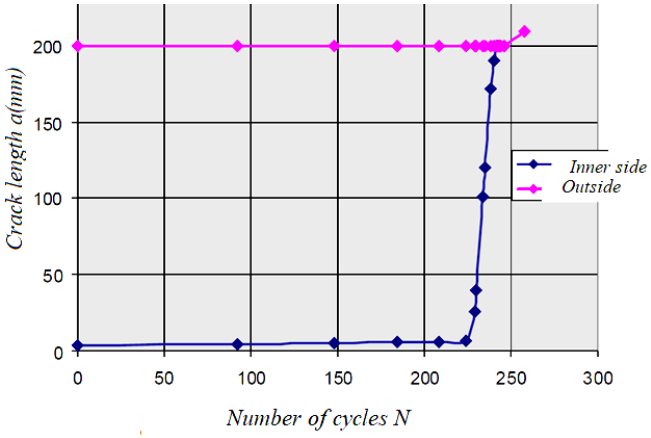

Figure 8. Crack length *a* vs. and number of cycles *N* for 100 propagation steps.

CONCLUSION

According to all the presented results, the following conclusions can be drawn.

- Based on prior verification by FEM, the efficiency of the XFEM is demonstrated by comparing numerical and analytical results in the case of 3D simulation of the fatigue crack growth in the oil rig test pipe.
- Analytical expressions for stress intensity factors are probably not adequate and should be corrected for relatively long cracks.

REFERENCES

1. Sedmak, A., Ković, M., Kirin, S. (2022), *Structural integrity - historical content*, Technical Gazette, 29(5): 1770-1776. doi: 10.17559/TV-20220321074430
2. Zaidi, R., *Application of fracture mechanics parameters to residual life assessment of welded pipes exploitation under fatigue loading*, Ph.D. Thesis, University of Belgrade, Faculty of Mechanical Engineering, Belgrade, 2021.
3. Iqbal, H., Tesfamariam, S., Haider, H., Sadiq, R. (2017), *Inspection and maintenance of oil & gas pipelines: a review of policies*, Struct. Infrastruct. Eng., Maint. Manag. Life-Cycle Des. Perf. 13(6): 794-815. doi: 10.1080/15732479.2016.1187632
4. Gabbar, H.A., Kishawy, H.A. (2011), *Framework of pipeline integrity management*, Int. J Proc. Syst. Eng. 1(3-4): 215-236. doi: 10.1504/ijpse.2011.041560
5. Dawotola, A.W., Van Gelder, P.H.A.J.M., Vrijling, J.K. (2009), *Risk assessment of petroleum pipelines using a combined Analytical Hierarchy Process - Fault Tree Analysis (AHP-FTA)*, In: Proc. 7th Int. Probabilistic Workshop, Delft, Netherlands, vol. 13, 2009, pp.491-501.
6. Lazić-Vulićević, Lj., Rajić, A., Grbović, A., et al. (2016), *Fatigue life prediction of casing welded pipes by using the extended finite element method*, Frattura ed Integrità Strutturale, 10(36): 46-54. doi: 10.3221/IGF-ESIS.36.05
7. Šarkoćević, Ž., Arsić, M., Međo, B., et al. (2009), *Damage level estimate of API J55 steel for welded seam casing pipes*, Strojarstvo, 51(4): 303-311.
8. Golubović, T., Sedmak, A., Spasojević-Brkić, V., et al. (2018), *Novel risk based assessment of pressure vessels integrity*, Tech. Gazette, 25(3): 803-807. doi: 10.17559/TV-20170829144636
9. Zaidi, R., Sedmak, A., Kirin, S., et al. (2020), *Risk assessment of oil drilling rig welded pipe based on structural integrity and life estimation*, Eng. Fail. Anal. 112: 104508. doi: 10.1016/j.engfailanal.2020.104508
10. Vučetić, I., Kirin, S., Sedmak, A., et al. (2019), *Risk management of a hydro power plant - fracture mechanics approach*, Tech. Gazette, 26(2): 428-432. doi: 10.17559/TV-20180618102041
11. Jeremić, L., Sedmak, A., Milovanović, N., et al. (2021), *Assessment of integrity of pressure vessels for compressed air*, Struct. Integr. Life, 21(1): 3-6.
12. Kirin, S., Sedmak, A., Zaidi, R., et al. (2020), *Comparison of experimental, numerical and analytical risk assessment of oil drilling rig welded pipe based on fracture mechanics parameters*, Eng. Fail. Anal. 114: 104600. doi: 10.1016/j.engfailanal.2020.104600
13. Lazić-Vulićević, Lj., Arsić, M., Šarkoćević, Ž., et al. (2013), *Structural life assessment of oil rig pipes made of API J55 steel by high frequency welding*, Tech. Gazette, 20(6): 1091-1094.
14. Newman, J.C., Raju, I.S. (1980), *Stress-intensity factors for internal surface cracks in cylindrical pressure vessels*, J Press. Ves. Technol. 102(4): 342-346. doi: 10.1115/1.3263343
15. Wang, X., Lambert, S.B. (1996), *Stress intensity factors and weight functions for longitudinal semi-elliptical surface cracks in thin pipes*, Int. J Pres. Ves. Pip. 65(1): 75-87. doi: 10.1016/0308-0161(94)00160-K